JOURNAL OF MATERIALS SCIENCE 24 (1989) 1827–1834

The relation between microstructure and ionic conductivity of hot-pressed β-Al_2O_3

J. L. SHI, J. H. GAO, Z. X. LIN
Shanghai Institute of Ceramics, Academia Sinica, Shanghai, People's Republic of China

The microstructure variation of β-Al_2O_3 with different compositions during hot-pressing and its effect on ionic conductivity were studied. It is found that, besides the phase composition, the conductivity of hot-pressed β-Al_2O_3 materials of the same composition is also related to the measurement direction, microstructure and density. The resistivity in the direction parallel to hot-pressing is about three times higher than that perpendicular to the hot pressing. The pores in the material are particularly detrimental to the ionic conduction. It was observed that the shape of complex impedance plane spectrum changed with measurement temperature and such change was affected by chemical composition and sample preparation condition. This phenomenon is explained successfully with the help of the ideal equivalent circuit of polycrystalline fast ionic conductor and the results of the conductivity measurement of hot-pressed β-Al_2O_3.

1. Introduction

β-Al_2O_3 (including β-Al_2O_3 and β''-Al_2O_3) is a two-dimensional fast ionic conductor of layer structures [1–3]. Its fast ionic conduction characteristic has been extensively studied theoretically and is expected to be used widely in practice [4–6]. Therefore, great efforts have been made to fabricate the material and improve its performances. Raw material selection and powder preparation [7–9], sintering and annealing [10–14] have been reported to have various effects on material preparation and its properties. However, factors affecting material performances can be eventually attributed to chemical and phase composition, and microstructure. The investigation of chemical and phase composition of β-Al_2O_3 has been fully performed, but the relation between the microstructure (e.g. grain size, grain orientation, pore size and its content, pore location, etc.) and the properties of β-Al_2O_3 need further investigation [18].

It is well known that almost pore-free ceramics with fine grain size can be fabricated by hot pressing [19] and the desired grain size and pore content can be obtained with subsequent annealing. Thus it is convenient to study the relation between microstructure and properties with the help of the hot-pressing method. In addition, the hot-pressing method offers us a good possibility of investigating the grain orientation of non-isotropic materials. The hot-pressing of β-Al_2O_3 has been performed by several investigators [20–22], but the relation between microstructure and properties has not been fully investigated. The present paper aims to investigate the microstructure evaluation of β-Al_2O_3 during the hot-pressing and annealing processes and the effect of such a variation on the ionic conductivity.

2. Experimental details

γ-Al_2O_3 (99.97%), Na_2CO_3 (A.R.), $Mg(OH)_2 \cdot 4MgCO_3 \cdot 5H_2O$ (A.R.) and $Li_2C_2O_4$ (A.R.) were used as raw materials, and the γ-Al_2O_3 was converted to α-Al_2O_3 by calcining at 1250° C for 2 h before use in experiment. The four compositions were used in the experiment (Table I, the remaining content is Al_2O_3).

The β-Al_2O_3 powder was prepared by a solid state reaction. The raw materials were mixed by wet ball-milling in ethanol for 4 h with α-Al_2O_3 balls as the media. After being dried at 80° C and calcined at 1250° C for 2 h, the powders were wet ball-milled again for 24 h. Then, the prepared powders were hot-pressed in a mini-hot-pressing furnace made in our institute [23].

The conductivity of hot-pressed β-Al_2O_3 was measured by complex impedance method, the frequencies used ranged from 1 to 150 kHz. To polycrystalline ceramics, the ideal complex impedance plane is as shown in Fig. 1a [28]. Fig. 1c is the equivalent circuit of Fig. 1a, where R_b, R_{gb} are the resistance of grains and grain boundaries, respectively and; C_{gb}, C_{dl} are the capacity of grain boundary and impedance electrodes, respectively; and ω is angular frequency, respectively. the practical impedance plane is shown in Fig. 1b.

3. Results and discussion

3.1. Microstructure of β-Al_2O_3 during preparation

3.1.1. Microstructure of as hot-pressed β-Al_2O_3

β-Al_2O_3 powders with different Na_2O content requires a different hot-pressing tempereature [23]. Powders with Na_2O content of 9% (samples 2, 6 and 7) and 8% (sample 3) were hot-pressed at 1450° and 1500° C, respectively, and the pressure used in all the

0022–2461/89 $03.00 + .12

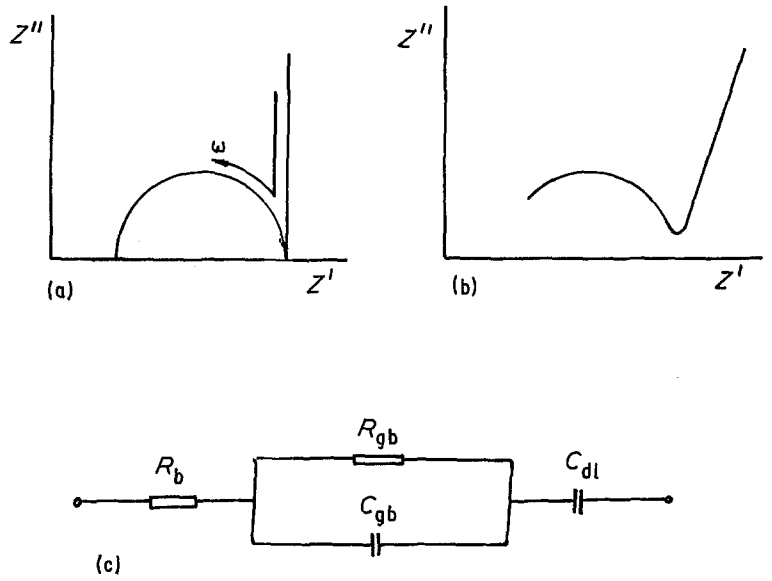

Figure 1 (a) Ideal and (b) practical impedance plane. (c) Equivalent circuit of Fig. 1a.

TABLE I Compositions used in the experiment (wt %)

Sample	2	3	6	7
Na_2O	9.00	8.00	9.00	9.00
MgO	2.50	2.50	1.25	–
Li_2O	–	–	0.40	0.80

experiments was 20 MPa. Under these conditions, the relative densities of hot-pressed β-Al_2O_3 were equal to or above 99%.

The microstructure of sample 3 is illustrated in Fig. 2, after being hot-pressed at 1500° C. It can be seen that the large grains of about 10–20 μm in length occured after hot-pressing in addition to the primary fine grains of about 2 μm. The other samples posses much more uniform grain size distribution than sample 3 and the grains are as fine as 2 μm or so after being hot-pressed at 1450° C. The microstructure of sample 2 is illustrated in Fig. 3 as an example.

3.1.2. Microstructure after annealing process

The microstructure of β-Al_2O_3 is affected greatly by the annealing step. Figs 4a–e are the microstructure of Li_2O doped sample 7 (SEM) after being annealed at different temperatures for 10 h. It can be seen that the grain size changed greatly as the annealing temperature increased. After being annealed at 1350° C, the grains showed little growth and the large grains are not obvious. At 1400° C, isolated large grains occurred. As the annealing temperature was elevated further, the large grains became larger and larger, and there were more and more of them. At 1450° C, there were only very few primary fine grains left. At 1550° C, the grain grew to as long as several tens of micrometres.

Fig. 5 shows the size change of the large grains of samples 2, 6 and 7, with annealing temperature shown on the x axis and grain size on the y axis. The computation method of grain size was to take the length, b, and width, c, of the 3 or 4 largest grains on every one of our 2 SEM microstructure photographs, and the average value of $(bc)^{1/2}$ was taken to be the large grain size (GS) of the samples (the C axis of β-Al_2O_3 is basically parallel to the hot-pressing direction and also perpendicular to the microstructure observation plane because of the preferred orientation of grains after hot-pressing). This computation method was approximate to some extent, but could indeed show the general trend of grain size variation. From the figure, it can be seen that the size variation is relatively small when the annealing temperature (T_a) is relatively low; but as T_a is raised to 1450° C, the grains began to grow rapidly, and the higher the T_a, the larger the growing rate of grain size. In addition, the content of large grains also increased and the primary fine grains became less and less as the large grains grew larger.

It can also be seen that there was a great difference between differently composed β-Al_2O_3. If the GS is

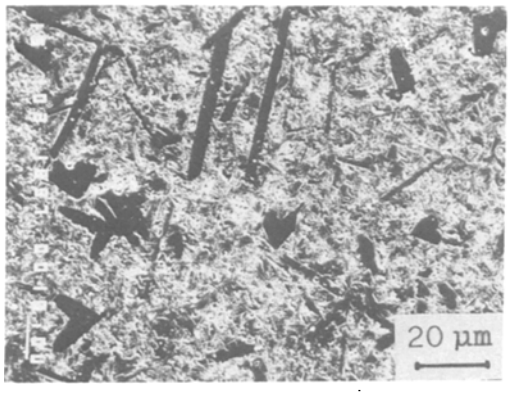

Figure 2 Microstructure of sample 3.

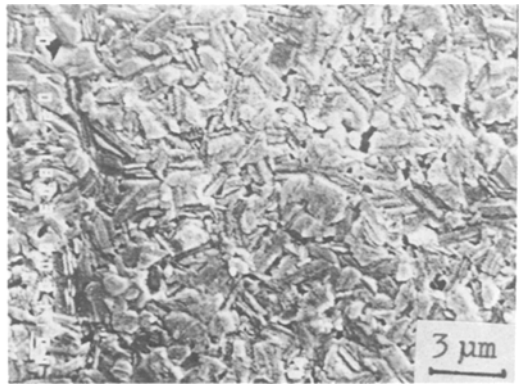

Figure 3 Microstructure of sample 2.

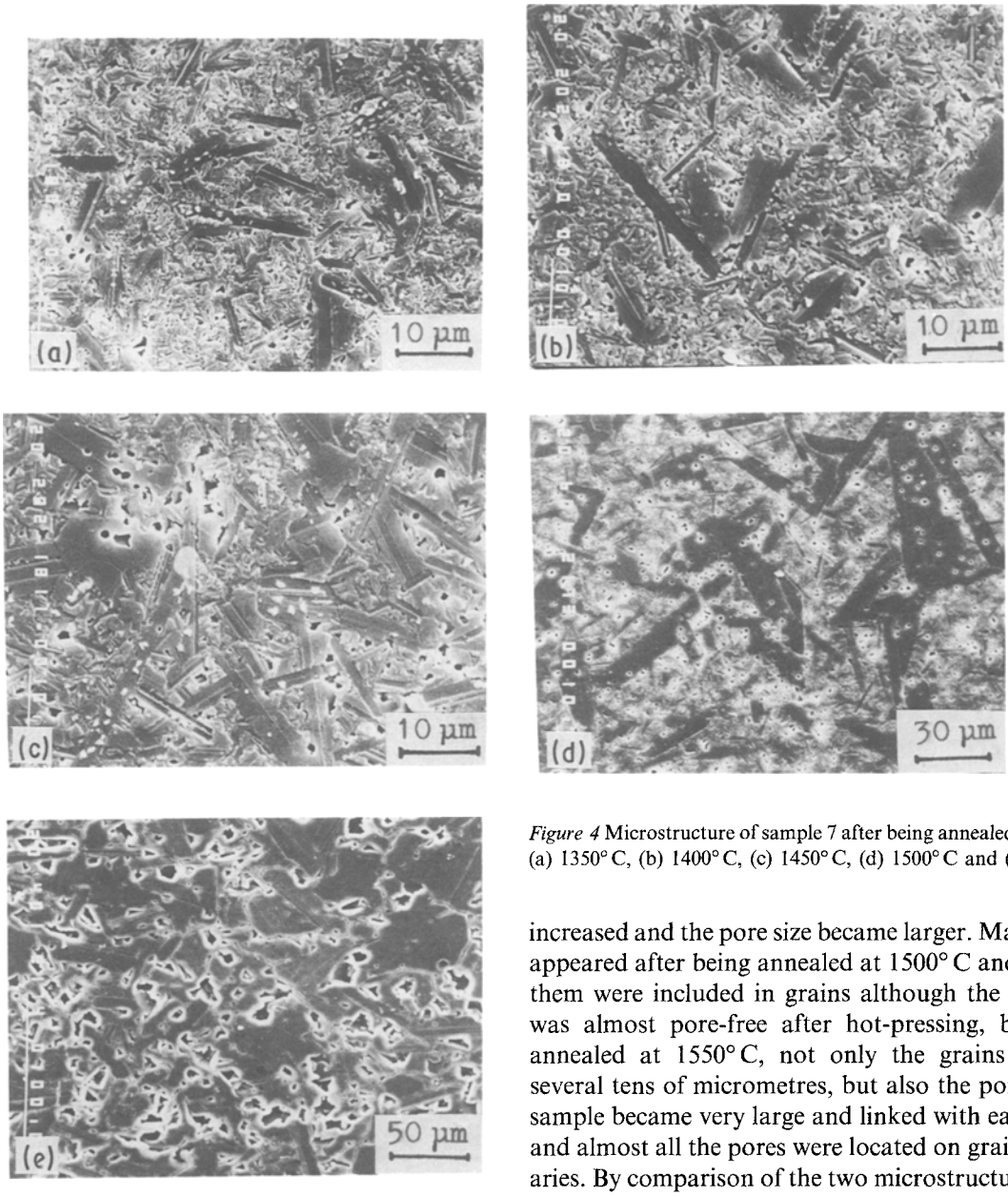

Figure 4 Microstructure of sample 7 after being annealed for 10 h at (a) 1350° C, (b) 1400° C, (c) 1450° C, (d) 1500° C and (e) 1550° C.

used to mean the grain size, the following result can be easily obtained from Fig. 5: GS (sample 7, Li_2O doped) > GS (sample 6, MgO and Li_2O doped) > GS (sample 2, MgO doped), under the same conditions. As the grains grew, the content of pores also increased and the pore size became larger. Many pores appeared after being annealed at 1500° C and most of them were included in grains although the sample 7 was almost pore-free after hot-pressing, but when annealed at 1550° C, not only the grains grew to several tens of micrometres, but also the pores in the sample became very large and linked with each other, and almost all the pores were located on grain boundaries. By comparison of the two microstructures it can be inferred that when T_a = 1500° C the rate of grain growth (i.e. migration rate of grain boundary) must be greater than that of pore migration [24–25]. However, as T_a was raised to 1550° C, the grains grew and came into contact with each other, the primary fine grains were deavoured, so further migration of grain

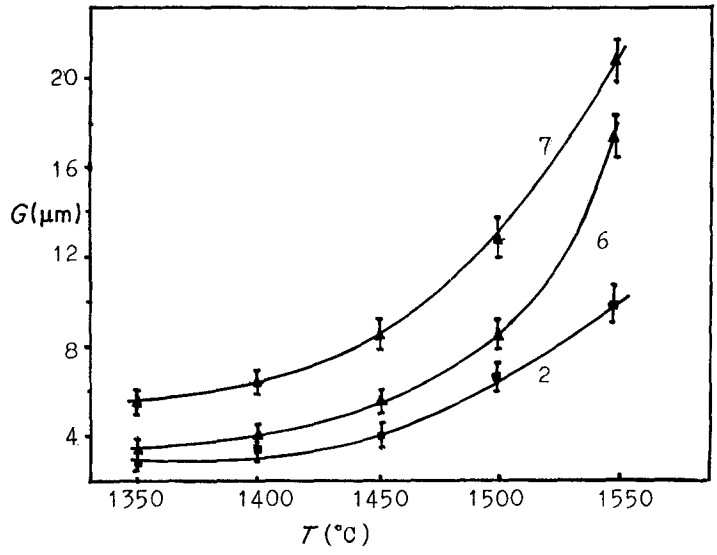

Figure 5 Large grain size plotted against annealing temperature.

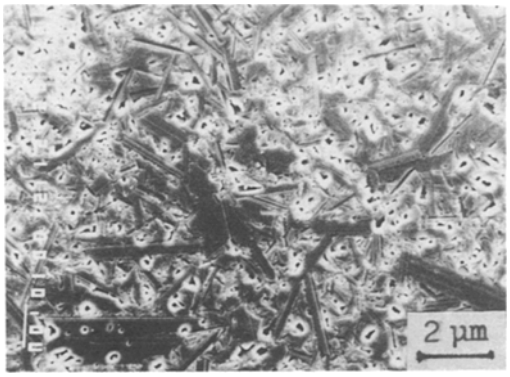

Figure 6 Microstructure of sample 2 after annealing at 1550° C.

boundaries became very difficult, the pores gathered at boundaries by diffusion from the midst of grains (Fig. 4(e)). There were fewer pores of sample 6 compared with sample 7, but when T_a = 1550° C, the pores also increased, and most of them were included in the grains. The porosity of sample 2 was much less than that of sample 7 under the same T_a, and most pores remained in the grains even when annealed at 1550° C (Fig. 6).

As the grain size and pore content increased, the densities of the samples decreased, as indicated in Fig. 7. The densities of all the samples 2, 6 and 7 decreased as T_a increased, especially at higher T_a, in agreement with microstructure observation.

3.2. Resistivity change with annealing temperature

The changes of microstructure and phase composition have a great affect on the ionic conductivity of β-Al_2O_3. The variation of $f(\beta)$ (the content of β phase, [26]) and resistivity with T_a are illustrated in Figs 8 and 9, respectively. When $T_a \leqslant$ 1500° C, $f(\beta)$ decreases as T_a increases, and at the same time the content of the β'' phase increases, so the resistivity also decreases to some extent, as the conductivity of β'' phase is better than that of the β phase [2, 3]. At the same time, the growth of grains is also effective on the reduction of the resistivity to some extent [18]. On the contrary as T_a increased from 1500 to 1550° C, although the grains grew larger and the phase composition remained basically constant, the resistivity increased greatly. The reason for this great increase can only be attributed to the great change of microstructure as T_a increases from 1500 to 1550° C, apart from the grain growth. As indicated in Figs 7, 4d and 4e, the densities decreased greatly and pores became big enough to compare with grain size when the samples were annealed at 1550° C (Fig. 4e), so it is possible to a large extent that the conduction passage of Na^+ in the layer structure of β-Al_2O_3 material are blocked by the pores located on the boundaries or in the grains, making the migration of Na^+ very difficult and the resistivity increases a great deal, particularly for the sample 7. From Fig. 4e showing sample 7, the microstructure was very relaxed, and pores were linked up with each other, so the migration of Na^+ was strongly impeded, the resistivity was especially large for the sample 7 when annealed at 1550° C. The observation of the effect of porosity on the conductivity of β-Al_2O_3 is in agreement with the work of Powers [27, 28].

In addition to pore and phase composition, the grain size would also affect the ionic conductivity. If the porosity in the material is assumed to be zero, and the grains are all cubes with side length equal to a and all grains compact ideally, then the volume content of grain boundaries (the width is thought to be h) α is as follows

$$\alpha = \text{Volume of grain boundary/Total volume}$$
$$= (6a \cdot h/2)/(a + h)$$
$$= 3a \cdot h/(a + h)$$

Generally speaking, $h \ll a$. So

$$\alpha \doteq 3h/a$$

So, in a certain range, the volume content of grain boundaries is inversely proportional to the grain size, and as we know, the resistivity of grain boundaries is much higher than that of grains at relatively lower temperature ($\sim$300° C), so under this condition, the larger the grains, the less the grain boundaries and the higher the conductivity.

3.3. Conductivity as a function of grain orientation

Fig. 10 is the microstructure (SEM) of the plane parallel to hot-pressing direction. From the figure the

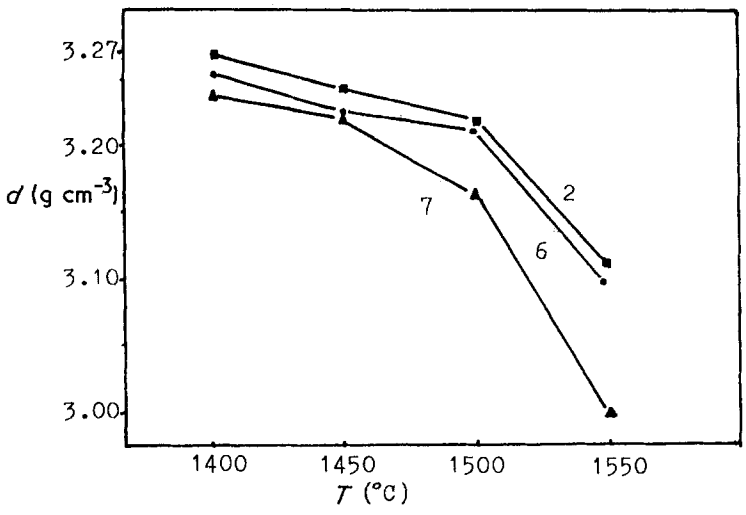

Figure 7 Sample density variation with T_a.

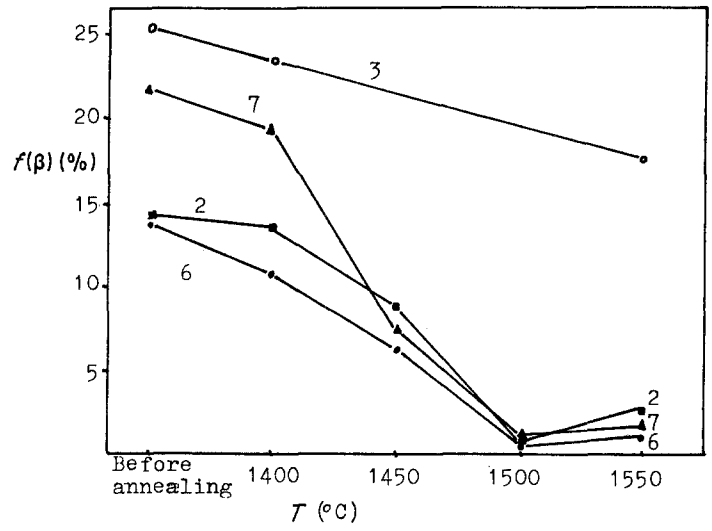

Figure 8 $f(\beta)$ plotted against annealing temperature.

preferred orientation of grains in the direction perpendicular to the hot-pressing direction can be seen clearly. The grain orientation of hot-pressed β-Al_2O_3 was also indicated with the XRD spectrum obtained on the different planes of hot-pressed samples. Fig. 11(1, 2 and 3) is the XRD spectrum obtained on the plane perpendicular to hot-pressing direction, powder (by the grinding of sintered sample) and on the plane parallel to hot-pressing direction, respectively. From the figure the diffraction peak of (0 0 6) plane (perpendicular to the C axis of β-Al_2O_3 crystal) in Fig. 11(1) is especially strong but it almost disappears in Fig. 11(3), and the strength of the peak in Fig. 11(2) is between the two of them. So it can be inferred that the C axis of the grains in hot-pressed β-Al_2O_3 material is parallel to hot-pressing direction on the whole for the (0 0 6) plane is vertical to C axis. Because of the two-dimensional ion conduction of β-Al_2O_3 grains, the orientation of the grains of hot-pressed β-Al_2O_3 would lead to the non-isotropism of the ionic conduction. Such differences are illustrated in Table II (sample preparation condition: 1450° C 20 MPa hot-pressing, 1400° C-10 h annealing. ∥HP and ⊥HP mean in the direction parallel and perpendicular to the hot-pressing).

From Table II, ϱ(∥HP) is about three times larger than ϱ(⊥HP), in agreement with Youngblood's report [29].

3.4. The shape of complex impedance plane as a function of microstructure

The ideal impedance plane of polycrystalline materials and its equivalent circuit of the measurement cell are shown in Figs 1a and 1c, and the practical impedance plane in Fig. 1b. Within the frequency range employed in the experiment, the shapes of impedance plane of different specimens under different T_a were in fact different, as shown in Fig. 12. Table III gives the measurement temperature (T_m) and T_a of every curve in Fig. 12.

As T_m increased, the curves gradually became straight and finally the half circuit disappeared, as the half circuit is the characteristic of the grain boundary capacity, so the disappearance of the half circuit is the disappearance of grain boundary capacity. However, for different T_a and different specimens, the temperature at which the half circuit disappears (denoted by T_{md}) differs. For the same sample, T_{md}(T_a = 1550° C), is higher than T_{md}(T_a = 1450° C), and for the same T_a, T_{md}(sample 2) is higher than T_{md}(sample 7).

For the half circuit capacity U characteristic of the grain boundary, so to make the half circuit disappear, the condensive reactance of grain boundaries, Z_{gb}, must be much larger than the resistance of grain boundaries R_{gb} (Fig. 1a), i.e. the following relation must be satisfied

$$Z_{gb}/R_{gb} \gg 1$$

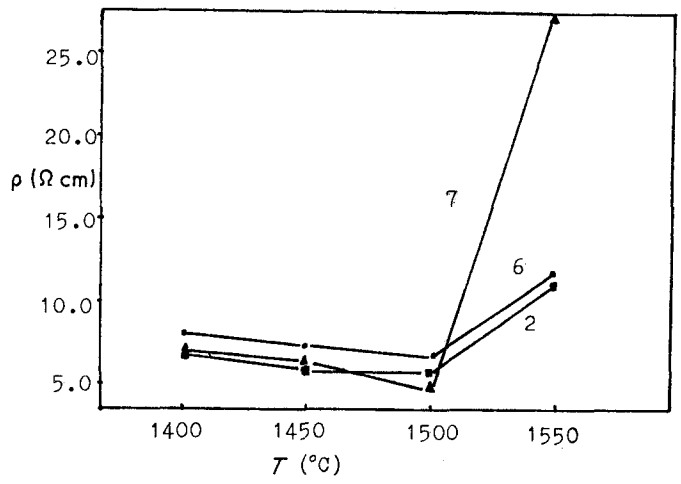

Figure 9 Resistivity plotted against annealing temperature.

TABLE II The conductivity non-tropism of hot-pressed Al_2O_3 (300° C)

Sample		2	6	7
ϱ	∥HP	25.0	26.3	17.1
(Ω cm)	⊥HP	6.90	9.03	6.50

As T_m increased, R_{gb} would decrease and Z_{gb} remain unchanged, so, the above relation will be satisfied at a certain T_m and the half circuit will disappear at T_m. If the resistance is signed to be, R, according to Fig. 9,

$$R, \text{ sample 7 } 1550°\text{C} > R, \text{ sample 7 } 1450°\text{C}$$

$$R, \text{ sample 2 } 1550°\text{C} > R, \text{ sample 2 } 1450°\text{C}$$

$$R, \text{ sample 7 } 1550°\text{C} > R, \text{ sample 2 } 1550°\text{C}$$

$$R, \text{ sample 7 } 1450°\text{C} > R, \text{ sample 2 } 1450°\text{C}$$

As $R = R_{gb} + R_b$, R_{gb} and R_b are the resistance of grain boundaries and grains respectively, and R_b can be thought to be the same for different samples and T_a at a given T_m we can obtain

$$(Z_{gb}/R_{gb}), \text{ sample 7 } 1550°\text{C}$$
$$< (Z_{gb}/R_{gb}), \text{ sample 7 } 1450°\text{C}$$
$$(Z_{gb}/R_{gb}), \text{ sample 2 } 1550°\text{C}$$
$$< (Z_{gb}/R_{gb}), \text{ sample 2 } 1450°\text{C}$$
$$(Z_{gb}/R_{gb}), \text{ sample 7 } 1550°\text{C}$$
$$< (Z_{gb}/R_{gb}), \text{ sample 2 } 1550°\text{C}$$
$$(Z_{gb}/R_{gb}), \text{ sample 7 } 1450°\text{C}$$
$$< (Z_{gb}/R_{gb}), \text{ sample 2 } 1450°\text{C}$$

The larger the Z_{gb}/R_{gb} for a given T_m, the smaller the T_{md}, so following relations can be obtained

$$T_{md}, \text{ sample 7 } 1550°\text{C} > T_{md}, \text{ sample 7 } 1450°\text{C}$$

$$T_{md}, \text{ sample 2 } 1550°\text{C} > T_{md}, \text{ sample 2 } 1450°\text{C}$$

$$T_{md}, \text{ sample 7 } 1550°\text{C} > T_{md}, \text{ sample 2 } 1550°\text{C}$$

$$T_{md}, \text{ sample 7 } 1450°\text{C} > T_{md}, \text{ sample 2 } 1450°\text{C}$$

The explanation is in agreement with the results of experiment.

4. Conclusions

The conclusions are as follows

(1) The microstructure of hot-pressed β-Al_2O_3 is affected greatly by annealing. Increasing annealing temperature will result in the quick growth of grains and the increase of porosity as well as pore size.

(2) The preferred orientation of grains leads to the ion conduction non-isotropism of hot-pressed polycrystalline β-Al_2O_3.

(3) The pores are very detrimental to the ion conduction of hot-pressed β-Al_2O_3 when the porosity has reached a certain value.

(4) The shape of complex impedance plane is also affected by microstructure. The larger the porosity, the higher the resistance of grain boundaries and the temperature at which the half circuit disappears.

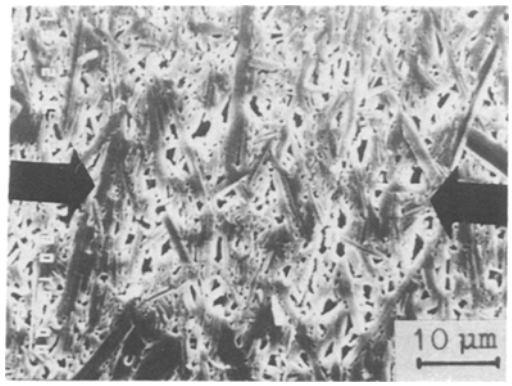

Figure 10 The grain preferred orientation of sample 2 (1450° C 20 MPa hot-pressing. 1550° C 10 h annealing, hot-pressing direction is indicated with black arrows).

References

1. N. WEBER and J. T. KUMMER, "Proceedings 21st Annual Sources Conference" Vol. 21. (1967) p. 42.
2. R. COLLONGUES, J. THERY and J. P. BOILOT, in "Solid Electrolytes", edited by P. Hagenmuller and W. V. Gool (Academic Press, New York, 1978) p. 253.
3. J. H. KENNEDY, in "Solid Electrolytes" (edited by S. Geller). Springer, Berlin (1977) p. 105.
4. M. B. SALAMON, "Physics of Superionic Conductors", (Springer, Berlin, 1979).
5. S. CHANDRA, "Superionic Solids, Principle and Application", (North-Holland, Amsterdam, 1981).
6. E. J. CAINS, in "Critical Material Problems in Energy Production", edited by C. Stain (Academic Press, New York 1976) p. 684.
7. R. KVADHKOR, A. YANAKIER and C. N. POULIEFF, *J. Mater. Sci.* **16** (1981) 2710.
8. G. E. YOUNGBLOOD, A. V. VIRKAR, W. R. CANNON and R. S. GORDON, *Amer. Ceram. Soc. Bull.* **56** (1977) 206.
9. D. W. JOHNSON, Jr., S. M. GRANSTATT, Jr. and W. W. RHODES, *ibid.* **58** (1979) 849.
10. M. L. MILLER, B. J. McENTIRE, G. R. MILLER and R. S. GORDON, *ibid.* **58** (1979) 522.

TABLE III The measurement temperatures of impedance curves in Fig. 12

Number	Sample	Annealing temperature (° C)	Measured temperature (° C)	Number	Sample	Annealing temperature (° C)	Measured temperature (° C)
1	7	1550	132	9	2	1550	60
2	7	1550	181	10	2	1550	136
3	7	1550	238	11	2	1550	205
4	7	1550	281	12	2	1550	242
5	7	1550	334	13	2	1550	330
6	7	1550	387	14	2	1450	50
7	7	1450	134	15	2	1450	106
8	7	1450	193	16	2	1450	180

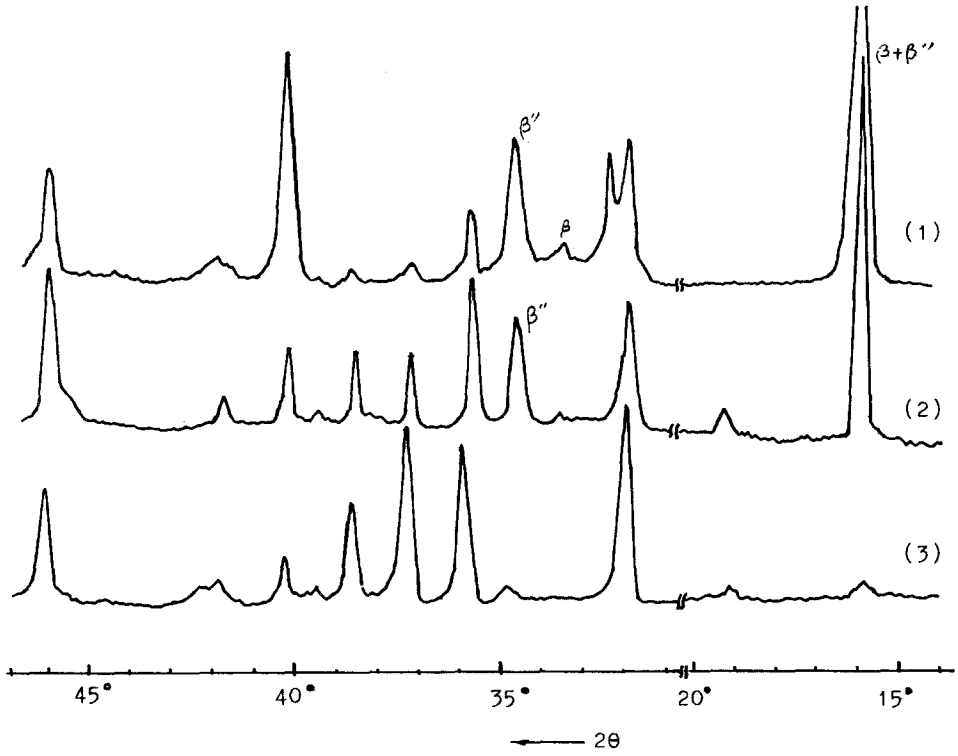

Figure 11 The XRD graphs of sample 2 (1450° C, 20 MPa, hot-pressing, 1400° C, 10 h annealing) (1) on the surface perpendicular to hot-pressing; (2) the powder (3) on the surface parallel to hot-pressing direction.

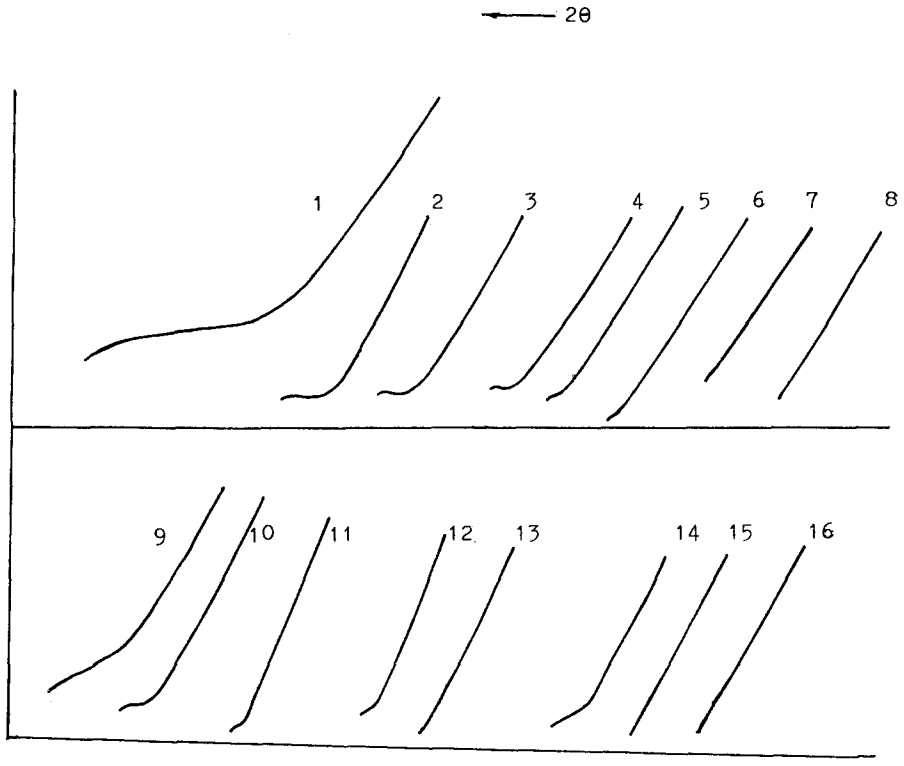

Figure 12 The shape change of complex impedance plane with annealing temperature (see Table III).

11. R. W. POWERS, *J. Electrochem. Soc.* **122** (1975) 490.
12. R. T. DIRSTINE, in "Fast Ion Transport in Solids" edited by P. Vashishta. J. N. Mundy and G. F. Shenoy, (Elsevier, Amsterdam, 1979) p. 79.
13. R. RIVIER and A. PELTON *Amer. Ceram. Soc. Bull.* **57** (1978) 183.
14. S. R. TAN and G. J. MAY, *Sci. Ceram.* **9** (1977) 103.
15. K. G. CHENG, Z. X. LIN, S. P. YANG and X. H. XU, *J. Chinese Silicate*, **14** (1984) 171.
16. K. G. CHENG, Z. X. LIN and X. H. XU, *ibid.* **12** (1984) 445.
17. A. TMAI and M. HARATA, *Jpn. J. Appl. Phys.* **11** (1972) 180.
18. A. V. VIRKAR, G. R. MILLER and R. S. GORDON, *J. Amer. Ceram. Soc.* **61** (1978) 250.
19. M. H. LEIPOLD, in "Ceramic Fabrication Processes" (edited by F. F. Y. Wang) Academic Press, New York (1976) p. 331.
20. A. V. VIRKER, T. D. KETCHAM and R. S. GORDON, *Ceram. Int.* **5** (1979) 66.
21. R. S. GORDON, B. J. McENTIRE, M. L. MILLER and A. V. VIRKAR, in "Processing of Crystalline Ceramics, edited by H. Palmour III, R. F. Davis and T. M. Hare (Plenum Press, New York, 1977) p. 405.
22. W. J. McDONOUGH, D. R. FLINN, K. H. STERN and R. W. RICE, *J. Mater Sci.* **13** (1978) 2403.

23. J. L. SHI, Z. Z. YANG and Z. X. LIN, *J. Chinese Silicate Soc.* **15** (1987) 233.
24. R. J. BROOK, in "Ceramic Fabrication Processes", edited by F. F. Y. Wang (Academic Press, New York, 1976) p. 331.
25. D. S. YAN, *J. Chinese Silicate* **9** (1981) 64.
26. A. PEKARSKY and NICHOLSON, *Mater. Res. Bull.* **15** (1980) 1517.
27. R. W. POWERS and S. P. MITTOD, in "Solid Electrolytes", edited by p. Hogen Muller and W. V. Goal (Academic Press, New York, 1978) p. 128.
28. R. W. POWERS and S. P. MITOFF, *J. Electrochem. Soc.* **122** (1975) 226.
29. G. E. YOUNGBLOOD, G. R. MILLER and R. S. GORDON, *J. Amer. Ceram. Soc.* **61** (1978) 86.

Received 23 November 1987
and accepted 29 April 1988